Hindawi
Journal of Chemistry
Volume 2018, Article ID 2124845, 12 pages
https://doi.org/10.1155/2018/2124845

Research Article

Kinetic Study of the Bioadsorption of Methylene Blue on the Surface of the Biomass Obtained from the Algae *D. antarctica*

Jhonatan R. Guarín,[1] Juan Carlos Moreno-Pirajan,[1] and Liliana Giraldo[2]

[1]*Department of Chemistry, Sciences Faculty, Research Group in Porous Solids and Calorimetry, University of the Andes, Bogota 111711, Colombia*
[2]*Departamento de Química, Facultad de Ciencias, Universidad Nacional de Colombia, Bogota 111321, Colombia*

Correspondence should be addressed to Juan Carlos Moreno-Pirajan; jumoreno@uniandes.edu.co

Received 9 March 2018; Revised 17 April 2018; Accepted 22 April 2018; Published 14 June 2018

Academic Editor: Carlos A. Martínez-Huitle

Currently, there is a great pollution of water by the dyes; due to this, several studies have been carried out to remove these compounds. However, the total elimination of these pollutants from the aquatic effluents has represented a great challenge for the scientific community, for which it is necessary to carry out investigations that allow the purification of water. In this work, we studied the bioadsorption of methylene blue on the surface of the biomass obtained from the algae *D. antarctica*. This material was characterized by SEM and FTIR. To the data obtained in the biosorption experiments, different models of biosorption and kinetics were applied, finding that the best fit to the obtained data is given by applying the pseudo-second-order models and the Toth model, respectively. It was also determined that the maximum adsorption capacity of MB on the surface of the biomass is 702.9 mg/g, which shows that this material has great properties as a bioadsorbent.

1. Introduction

Water pollution by various industries is the main problem the world is facing these times. Among these pollutants are the dyes [1, 2]; their world production per year is approximately 7×10^5 MT, and around 10 to 15% of the dyes used are dumped in waste water [3]. Synthetic dyes are more difficult to remove than natural dyes [4], and this is due to their complex aromatic structure, which gives them stability against air and light [1]. They can easily transport within the aqueous environment due to their high solubility in water [5]. They affect the aquatic autotrophs by restricting their photosynthetic efficiency because only limited sunlight is allowed to penetrate due to their colour; their toxic effect spreads along the food chain, and they are conserved for long periods deteriorating animal and human health [1].

Methylene blue (MB) is a cationic dye with broad applications such as dye for paper, hair, and cotton and filters for medical surgery [2] among others. This pollutant not only deteriorates water quality but also significantly affects the environment and human health [6]. It has been shown that, in humans, it causes vomiting, lightheadedness, cyanosis, jaundice, tissue necrosis [2], increased heart rate, vomiting, shock, and tetraplegia [7]. Therefore, there is a need to eliminate this dye present in wastewater or industrial effluents to ensure a safer environment [2]. This and the other dyes are difficult to degrade biologically, so the studies aimed at removing these contaminants present in aqueous solution are important and must be carried out [8, 9] to reduce environmental damage and human health.

Various technologies, including adsorption, flocculation, membrane filtration, electrolysis, biological treatments, oxidation [10], sedimentation, membrane separation, reverse osmosis [8], and photocatalytic degradation [11], have been adopted to remove dyes from sewage water. Among the mentioned treatments, adsorption has some advantages because the adsorbents are inexpensive, are available, are simple to use, and have high efficiency [8] and their design is simple [3]. However, the total removal of MB from the wastewater has not been achieved; therefore, it is necessary to continue with the studies to discover new bioadsorbents [6].

Many adsorbents have been studied to reduce the concentration of the dyes present in aqueous solutions, among which the activated carbon stands out for its high efficiency; however, its manufacture and regeneration involve a high cost. So, they have discovered and applied other natural adsorbents such as natural coal, chitin, chitosan, fly ash, wood sawdust, and rice husk [8].

Adsorption using biomass is considered a potential technique for the removal of contaminants present in water, and the advantage of using this adsorbent is that it is more economical than commercial adsorbents [12]. The scope of this research is to perform the kinetic study of the MB adsorption on the surface of the biomass obtained from the algae *D. antarctica* and to determine the capacity of adsorption of the contaminant (MB) by the bioadsorbent. To understand the mechanism of adsorption of this process, different kinetic and adsorption models were applied to the obtained data. Additionally, traditional instrumental techniques were used to characterize the bioadsorbent.

2. Materials and Methods

2.1. Preparation of the Biomass. Biomass brown alga was collected from the Chilean coast, for preparing samples of fresh alga washed with distilled water to remove impurities, and dried at 40°C using an oven (Memmert, Germany) for 72 hours; once the drying process was finished, the material was cut into small pieces, before being grounded, and the dried biomass was sieved to a particle size of 500–1000 μm. This material was used in all experiments [13].

2.2. Characterization. In order to evaluate the properties of the biomass surfaces obtained from the algae *D. antarctica*, which allow MB adsorption to be effective, this material was characterized by the techniques provided below.

2.2.1. Infrared Spectroscopy. The data of the IR spectra of the biomass before and after the adsorption of MB were recorded using an instrument SHIMADZU IRTracer-100. The pressed granules were prepared by grinding the biomass and mixing it with KBr in an agate mortar. The spectral data were recorded at wavenumber values between 4000 and 500 cm^{-1}.

2.2.2. Scanning Electron Microscopy. This technique was used to observe the morphology of the biomass surface before and after the MB adsorption process in a JEOL JSM-6490LV unit. For the SEM analysis, the sample obtained after the MB adsorption process was separated from the solution and dried at a temperature of 120°C for 5 h. Before carrying out this analysis, the surface of the biomass was coated with gold using the sputtering method to obtain a conductive surface.

2.3. Studies of the Biosorption of the Function of the pH. For the determination of the optimum pH of biosorption, methylene blue solutions of 50 ppm were prepared, whose pH was adjusted to values of 3, 5, 7, 9, and 11, after which the biomass was added in a ratio of 1 g/L, the samples were left in constant agitation for a period of 15 hours, and the MB concentration was determined at the beginning and end of the bioadsorption process by UV-Vis spectroscopy at a wavelength of 664 nm in a GENESYS 5 spectrophotometer.

2.4. Studies of Adsorption Kinetics. To prepare the kinetic studies, solutions of 25, 50, 100, 150, and 200 ppm of MB were prepared. According to the results obtained in Section 3.2, the optimum pH value of adsorption must be above 5; therefore, the pH of the solutions was adjusted to a value of 10 using 0.1 M·HCl and NaOH solutions. After this, the biomass was added in a ratio of 1 g/L, the samples were left in agitation, and aliquots were taken at 0, 5, 10, 15, 30, 60, 120, 240, 360, 480, and 560 minutes, to track the decrease in MB concentration present in the solution. Using (1), the values of q_t were determined for the different kinetic experiments carried out:

$$q_t = \frac{V(C_0 - C_t)}{m}, \quad (1)$$

where q_t is the amount of MB adsorbed per gram of the sample (mg/g) in time (t) of the adsorption process, C_0 is the initial concentration of the solution (mg/L), C_t is the concentration of the solution in time (t) of the adsorption process (mg/L), V is the initial volume of the solution, and m is the biomass added to the different solutions [14].

2.5. Studies of Equilibrium in the Solid-Liquid Interface. To understand the mechanism of adsorption of methylene blue on the surface of the biomass, solutions were prepared with initial concentrations of 25, 50, 100, 150, 200, 400, 600, 800, 100, and 1400 ppm of this contaminant; the pH of the solutions that were in the concentration range of 25 to 200 ppm was adjusted to a value of 10, and the pH value of the solutions that were in the concentration range of 400 to 1400 ppm was not adjusted since the pH value of these solutions was above 5. In Section 3.2, it was determined that, at basic pH values, the adsorption capacity of MB on the surface of the biomass is constant, so it was decided not to make adjustments to the pH value of these solutions.

The samples were left in agitation for 18 hours; using UV-Vis spectroscopy, the concentration of these solutions was determined at the beginning and at the end of the process. Using (2), the MB's adsorption capacity was determined by the biomass when the solution is in equilibrium at the end of this process:

$$q_e = \frac{V(C_0 - C_e)}{m}, \quad (2)$$

where q_e is the amount of MB adsorbed per gram of the sample (mg/g) at equilibrium and C_e is the concentration of MB in equilibrium (mg/L). The data obtained were adjusted to the models of Freundlich, Langmuir, Redlich–Peterson, Sips, and Toth, to understand the

mechanism of adsorption of MB which takes place on the surface of biomass [14].

2.6. Thermodynamic Studies of the Kinetics of Adsorption. Speed laws are essential in any study of biosorption because they provide an exact expression during the duration of the reaction [15]. Then, the models used in the present study are described below.

2.6.1. Pseudo-First-Order and Pseudo-Second-Order Models. There are several models of kinetics, but in general, the most used and compared ones are the pseudo-first-order and pseudo-second-order kinetic models. The pseudo-first-order kinetic model was proposed for the first time at the end of the 19th century by Lagergren, and the speed constant when using this model is denoted as K_1 [16]. The pseudo-second-order kinetic model was introduced for the first time in the mid-80s, but its recognition increased in the year of 1999 when Ho and McKay [17] took data from experiments reported in the literature and determined that the best fit to the data coming from all the systems studied was given by applying the pseudo-second-order model. After this publication came to light, the speed constant K_2 has become more popular since in most studies, it has been found that the data obtained fit this model; for this reason, the original article has more than 6000 citations, a figure that has increased exponentially over the course of the time [18], and the equations of these two models are presented below.

A pseudo-first-order model is given as follows:

$$\log\left(1-\frac{q_t}{q_e}\right)=\frac{k_1}{2.303}t, \tag{3}$$

where q_t is the concentration of the adsorbed phase at a certain time of the adsorption process, q_e is the concentration of the adsorbed phase at the end of equilibrium with the solid present in suspension, t is the time that has elapsed since the process of adsorption began, and k_L is the Lagergren constant (s^{-1}). The pollutant adsorption rate is proportional to the time that has elapsed since the adsorption process began; for $T=0$, the value of $q_t=0$; once equilibrium has been reached, the value of $q_t \approx q_e$ [19].

A pseudo-second-order model is given as follows:

$$\frac{t}{q_t}=\frac{1}{k_2 q_e^2}+\frac{1}{q_e}t. \tag{4}$$

When t approaches zero, the bioadsorption velocity q_t/t becomes the initial bioadsorption velocity, and the data obtained in the kinetic study are adapted to the pseudo-second-order model by plotting the graph of t/q_t versus t. The linear relationship obtained will allow the calculation of q_e, k_2, and $k_2 q_e^2$ without previously knowing any parameter [20].

2.6.2. Modified Pseudo-First-Order Model. This kinetic model is useful when the experimentally obtained data do not conform to the pseudo-first-order and pseudo-second-order kinetic models and the model of intraparticle diffusion. In this new model, the pseudo-first-order equation is modified by the speed constant as observed in the following equation [21]:

$$\ln\left(1-\frac{q_t}{q_e}\right)+\frac{q_t}{q_e}=-k_m t. \tag{5}$$

Since $q_t < q_e$, this equation implies that the velocity constant k_1 is minimal when equilibrium has been reached [21].

2.6.3. Elovich Model. It has been found that Elovich's empirical adsorption model has broad applicability for numerous adsorption systems. This model is based on the assumption of energetic heterogeneity of the adsorption sites in the form of rectangular distribution [22].

The kinetic model of Elovich is reported as follows:

$$q_t=\frac{1}{\beta}\ln(\alpha\beta)+\frac{1}{\beta}\ln t, \tag{6}$$

where α is the initial adsorption rate of the Elovich equation ($mg \cdot g^{-1}\ min^{-1}$) and β is the adsorption constant of the model ($g \cdot mg^{-1}$) [15]; it is related to the adsorption energy [23].

The Elovich equation can be linearized by assuming $\alpha\beta t >> t$ and that $Q=0$ at $t=0$ and that $Q=Q_t$ for a time $t=t_t$ [24]. Under these conditions, a graph of q_t versus ln (t) shows a linear relationship with a slope of ($1/\beta$) and an intercept of ($1/\beta$) ln ($\alpha\beta$) [15].

This equation has been used by some authors to describe the kinetics of adsorption of contaminants in natural adsorbents, prepared or modified, which found that the best behavior of the data obtained is given when applying this model. But in spite of the utility of the Elovich equation in the estimation of the biosorption kinetics, the study of other kinetic models must be carried out, since these can present, in some cases, marginally superior correlation coefficients in the kinetics of adsorption of chemical substances [15].

This equation is also used to describe reaction mechanisms such as solute diffusion in the solution or interface phase, surface activation, and deactivation. It is adequate to elucidate the process with significant changes of activation energy. In addition, the Elovich equation can also reveal the irregularity of data that other dynamic equations have ignored [25].

2.6.4. Intraparticle Diffusion Model. According to chemical reaction fundamental theory, intraparticle diffusion becomes a limiting factor to the overall reaction rate when the catalyst particle size is too large and/or the intrinsic reaction rate is too fast compared to the diffusion rate of reacting molecules inside the catalyst pores. The degree of inhibition resulting from the overall velocity depends on the combination of particle size and shape, intrinsic reaction velocity, and diffusion rate [26].

According to literature [26], if the rate-limiting step is intraparticle diffusion, then the amount adsorbed at any time t should be directly proportional to the square root of the contact time t and pass through the origin.

Table 1: The names and equations of applied error functions [7].

Error function	Definition	Equation
RMSE	$\sqrt{\frac{1}{n-2}\sum_{I=1}^{N}(q_{e,exp}-q_{e,isotherm})^2}$	(9)
X^2	$X^2=\sum_{1}^{N}\frac{(q_{e,exp}-q_{e,isotherm})^2}{q_{e,isotherm}}$	(10)
ERRSQ	$\sum_{i=1}^{N}(q_{e,exp}-q_{e,isotherm})_i^2$	(11)
HYBRD	$\sum_{i=1}^{N}\left[\frac{(q_{e,exp}-q_{e,isotherm})^2}{q_{e,exp}}\right]_i$	(12)
MPSD	$\sum_{i=1}^{N}\left[\frac{(q_{e,exp}-q_{e,isotherm})}{q_{e,exp}}\right]_i^2$	(13)

The intraparticle diffusion model is reported as follows:

$$\mathrm{Log}\, q_t = \log k_{ip} + 0.5\, \log t, \tag{7}$$

where k_{ip} is the intraparticle diffusion rate constant (mg/g/min$^{-0.5}$) [14].

The graph of q_t against 0.5 log t should produce a straight line with a positive intercept for the adsorption process controlled by intraparticle diffusion. The constant K is determined from the intersection with the Y-axis, and the high values of this parameter are related to a great adsorption speed [27].

2.6.5. Film Diffusion Model. The film diffusion model is reported as follows:

$$\ln\left(1-\frac{q_t}{q_e}\right) = -k_F t + A, \tag{8}$$

where k_F (1/min) and A are the constants of the film diffusion model [28].

In order to minimize the error distribution between experimental equilibrium data and values obtained by isotherm correlations, different error functions are generally applied. This goal of minimizing the error distribution is achieved by finding the minimum value of certain error functions or maximizing them depending on the definition of the selected error function. Therefore, choosing an error function seems indispensable in order to evaluate the best fit isotherm to the experimental equilibrium data [7]. In the present investigation, five different error functions (Table 1) were used to establish with certainty the isotherm of the kinetic model that presents the best adjustment of the adsorption of methylene blue on the surface of the algae *D. antarctica*.

2.7. Thermodynamic Studies of Bioadsorption

2.7.1. Model of Freundlich. The Freundlich model is described by an empirical equation used for systems with a high degree of heterogeneity. In this model, it is assumed that adsorption occurs at different sites and the formation of multilayers occurs with different adsorption energies. This leads to an exponential decrease in energy as the coverage of the surface originates [29].

The model of the Freundlich isotherm is reported as follows:

$$q_e = K_f C_e^{(1/n_f)}, \tag{14}$$

where q_e (mg $*$ g^{-1}) is the capacity of bioadsorption of the metal by the algae *D. antarctica* in the balance, C_e (mg $*$ L^{-1}) is the concentration of the metal in the equilibrium, and K_f (mg $*$ g^{-1} (L $*$ mg^{-1})$^{(1/n_f)}$) and n_f (dimensionless) are the constants of the Freundlich isotherm and are related to the capacity of biosorption and intensity, respectively; Freundlich's constant (n_f) depends on the adsorption capacity, and it is used to evaluate the favourability of adsorption. The values of n_f between 2 and 10 indicate a high adsorption capacity, while values between 1 and 2 indicate a moderate adsorption capacity and values less than 1 indicate a small adsorption capacity [30].

2.7.2. Langmuir Model. The Langmuir model is based on the assumption that adsorption occurs on a surface with homogeneous sites, where each molecule of the adsorbate occupies an adsorption site, and maximum adsorption occurs with the formation of the complete monolayer, in which there is migration of the adsorbate molecules on the surface of the adsorbent [31].

The model of the Langmuir isotherm is reported as follows:

$$q_e = \frac{q_m K_L C_e}{1 + K_L C_e}, \tag{15}$$

where q_m (mg $*$ g^{-1}) is the maximum adsorption capacity of the bioadsorbent and K_L (L $*$ mg^{-1}) is the Langmuir equilibrium counterrelated to bioadsorption energy.

2.7.3. Sips Model. The two models of previous isotherms have been widely used to analyze the biosorption of various pollutants present in aqueous solutions. The Sips model simultaneously involves the Freundlich and Langmuir models, has three parameters taken from the theory of these models [32], and has a greater capacity to describe the biosorption equilibrium.

The model of the Sips isotherm is reported as follows:

$$q_e = \frac{q_m (K_s C_e)^{(1/n_s)}}{1 + (K_s C_e)^{(1/n_s)}}, \tag{16}$$

where K_s is the Sips count in equilibrium and n_s (dimensionless) is the heterogeneity factor; a value of n_s close to or equal to 1 is given in bioadsorbents with homogeneous active sites [33], while a value of n_s close to 0 is given in biosorbents with heterogeneous active sites [34].

2.7.4. Toth Model. In the Toth model, an asymmetric quasi-Gaussian energy distribution is assumed, where most of the sites have a lower adsorption energy than the energy peak of maximum adsorption [29]. Toth modifies the Langmuir equation in order to reduce the error between the experimental and predicted values of adsorption equilibrium. This model is best suited for heterogeneous systems in which multiple layer adsorption occurs. The exponent of the

isotherm of Toth (n_{T_0}) is related to the heterogeneity of the surface; if it is equal to the unit, the Toth model is reduced to the Langmuir model. This correlation is applied for liquid-solid adsorption [35].

The model of the Toth isotherm is reported as follows:

$$q_e = Q_m C_e \left(b_{T_0} + C_e^{n_{T_0}}\right)^{\left(-1/n_{T_0}\right)}, \quad (17)$$

where b_{T_0} and n_{T_0} are constants of the model.

2.7.5. Redlich–Peterson Model. The Redlich–Peterson isotherm is an empirical model with no theoretical basis, which contains undefined empirical parameters (K_R and α_R). This model can be applied for homogeneous and heterogeneous surfaces and does not follow the ideal monolayer adsorption; as a consequence, this model provides the best approximation of the experimental data. However, the main disadvantage of this model is the lack of estimation of the maximum adsorption capacity. Another disadvantage when applying this model is that it does not adjust to the experimental data; in the trials, the dose of some variables has varied, since the constant α_R depends on the dose of the variables studied [22]. It should also be noted that this model includes the characteristics of the Langmuir and Freundlich isotherms in a single equation.

The Redlich–Peterson isotherm model is reported as follows:

$$q_e = \frac{K_{RP} C_e}{1 + \alpha_{RP} C_e^g}, \quad (18)$$

where K_{RP} is the constant of the Redlich–Peterson model (L/g), α_{RP} is another constant of the Redlich–Peterson model $(mg/L)^{-g}$, and g is the exponent of this model and must be between $0 < g \leq 1$.

When $g = 1$, the Redlich–Peterson equation becomes the Langmuir equation:

$$q_e = \frac{K_{RP} C_e}{1 + a_{RP} C_e}. \quad (19)$$

When $g = 0$, the Redlich–Peterson equation becomes Henry's law (20) [35]:

$$q_e = \frac{K_{RP} C_e}{1 + a_{RP}}. \quad (20)$$

3. Results

3.1. Characterization

3.1.1. Infrared Spectroscopy. The FTIR spectra before and after MB adsorption can be seen in Figure 1. In this analysis, several peaks assigned to the vibrations of the biomass functional groups were detected. Some of them are involved in MB adsorption, while others did not disappear, or their wavenumber shifted when this process was completed. The appearance of new peaks after the bioadsorption process was also observed due to the interaction between the functional groups of the bioadsorbent and the MB.

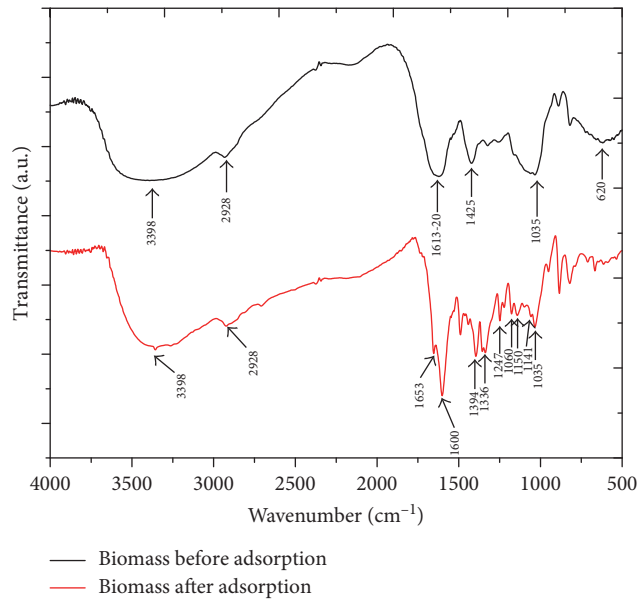

Figure 1: Infrared spectrum of the biomass of *D. antarctica* before and after the bioadsorption of MB.

The peaks at 3398 and 1613 cm^{-1} of the biomass before the adsorption process correspond to antisymmetric OH stretch vibrations [36, 37] and to the C=O bond present in the acids [36, 38], the peak located at 1425 cm^{-1} corresponds to primary alcohols [38], the peak at 2.936 cm^{-1} is due to the stretching vibrations of OH of carboxylic acids [39], the biomass adsorption band before and after adsorption of MB at a wavenumber of 1035 cm^{-1} is assigned to the CO present in the esters, and the peak at 1060 cm^{-1} can also be assigned to CO stretches [40].

The IR peaks of the MB that appeared after the adsorption process are described as follows: the peaks at 1600 and 1394 cm^{-1} correspond to vibrations of the aromatic ring and the CN bond, respectively, the peaks at 1336, 1141, and 1247 cm^{-1} are attributed to symmetric deformation of $-CH_3$ and the CN bond, respectively [37], the peaks at 1653 [39, 40], 1394, 1336, and 1141 cm^{-1} can be assigned to the vibrations of –C=C– of the stretch of the alkenes, to the C–C stretching in the aromatic ring, to the balancing of the CH alkanes, and to the wagging of the C–H ($-CH_2Cl$) of alkyl halides, respectively, the peak at 1247 cm^{-1} corresponds to the stretching of aliphatic amines [39], and the peak observed at 1150 cm^{-1} belongs to the vibration stretch of $-SO_3$ [41].

These observations clearly showed that the MB molecules were adsorbed on the surface of the biomass obtained from the algae *D. antarctica* and that the active functional groups of the biomass that participated in the binding of the MB molecules were –OH, CO, C=O, and –COO– representing, respectively, hydroxyl group, inorganic carbonates, and cyclic anhydride and carboxylic groups [38].

3.1.2. Scanning Electron Microscopy. This analysis was carried out in order to obtain a view of the morphology of the biosorbent surface. The obtained micrographs are presented in Figure 2.

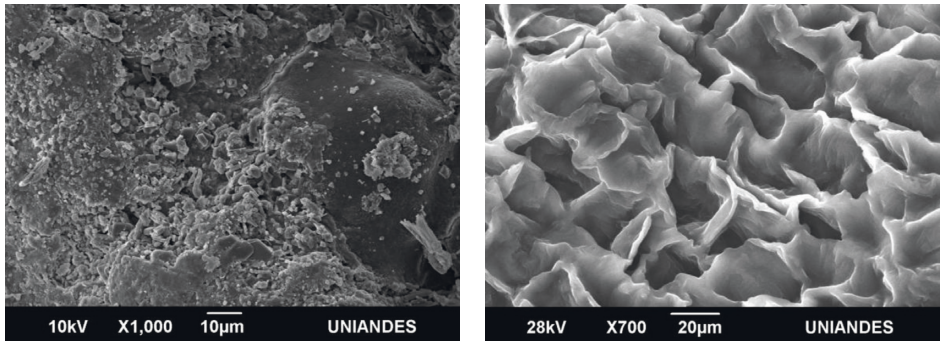

(a) (b)

Figure 2: SEM micrographs of the biomass (a) before and (b) after the biosorption process of MB.

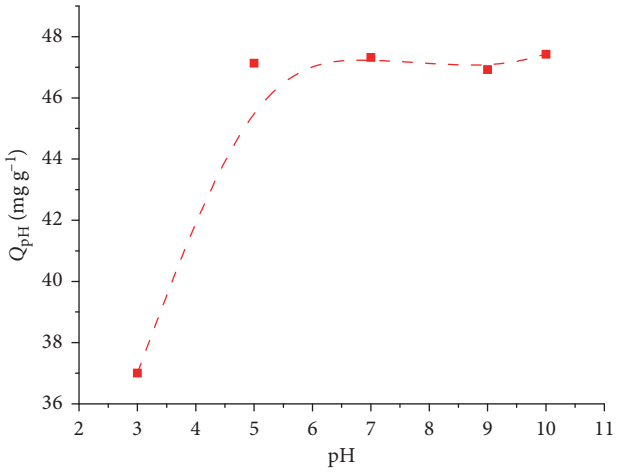

Figure 3: Effect of pH on bioadsorption of MB on the surface of the biomass of *D. antarctica*.

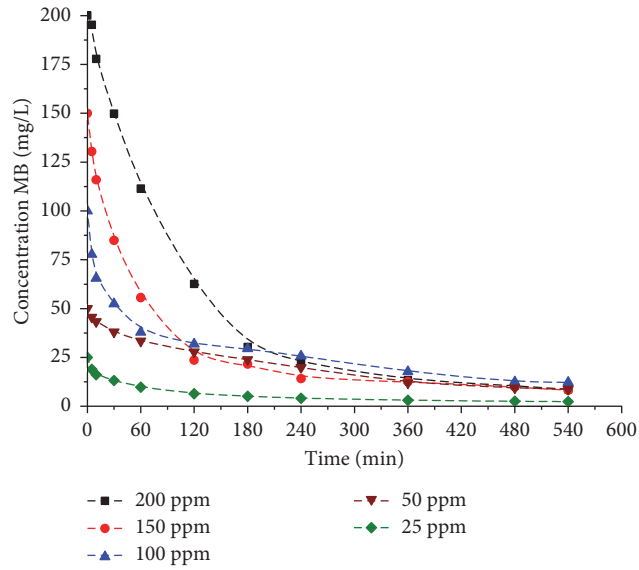

Figure 4: Effect of the concentration on the adsorption speed of MB on the surface of the biomass of *D. antarctica*.

Using this technique, it was determined that the pores present in the surface of the biomass are homogeneously distributed; however, there are areas in the surface that are not porous, so it is valid to say that a percentage of the porosity is distributed heterogeneously and it is worth mentioning. In addition, the MB adsorption process did not modify the surface of the biomass. In Figure 2(a), a part of the nonporous surface of the biomass is observed, while in Figure 2(b), the porous part of the biomass is observed, which retained its texture after the MB adsorption process. This is attributed mainly to the size of the methylene blue molecule, which is 0.84 nm [42], since each molecule of this contaminant interacts with a single active site present on the surface of the biomass; therefore, the pores of the biomass, having a diameter size greater than 50 μm, were not blocked during the biosorption process.

3.2. Determination of the Optimum pH for the Adsorption of Methylene Blue. The effect of pH on the adsorption of dyes is an important parameter. In Figure 3, the capacity of adsorption of MB by the biomass increased significantly when changing the pH value from 3 to 5, and this value was kept constant up to a basic pH corresponding to 11.

The chemical surface of an adsorbent has a great influence on the adsorption of an adsorbate, and this can be altered by modifying the initial pH value. Some authors have reported that, at low pH values, there is an electrostatic repulsion between the surface of the positively charged adsorbent and the cationic MB molecules, which inhibits the adsorption of this contaminant [4, 37, 43], because the ions of hydrogen compete with the MB molecule for the adsorption sites. As the pH increases, the surface of the biomass acquires a negative charge and a deprotonation of the surface is carried out which facilitates the adsorption of MB and therefore the capacity of adsorption of this pollutant by the biomass increases [37]. This is mainly because in the solution, the MB is positively charged; hence, its adsorption is more effective when the surface charge presents a negative value [44, 45]. Therefore, it was considered that a pH value of 10 was appropriate for carrying out the kinetic experiments.

3.3. Kinetics Models. In Figure 4, the larger the value of the initial concentration of MB, the more drastic the decrease in

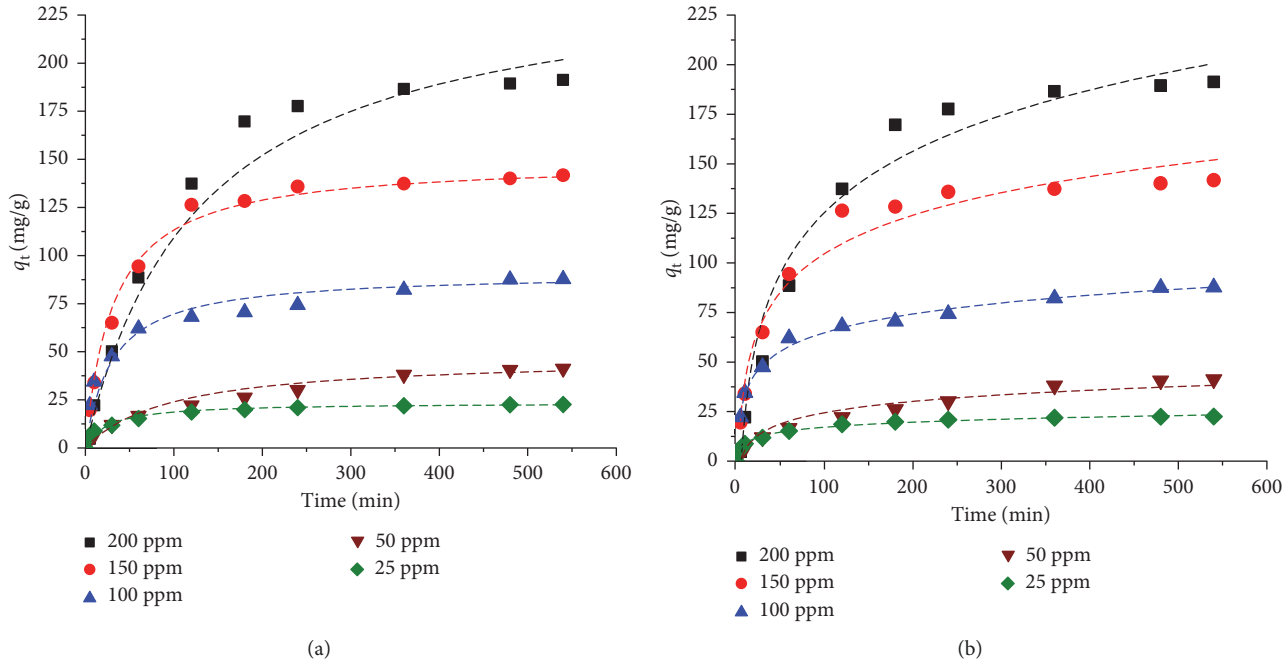

FIGURE 5: Result of applying the kinetic models used in the adsorption of MB on the surface of the biomass: (a) modified pseudo-first-order model; (b) Elovich model.

the value of its concentration, and as the time elapses, the change in concentration is less noticeable. In the first 180 minutes, the decrease in the MB concentration in the samples whose initial concentration was 200, 150, and 100 ppm is quite fast because the MB concentration remained above 20 ppm. However, after this time and smaller MB concentration values, the concentration changes are less noticeable. This is corroborated when observing that the decrease of the concentration of the contaminant in the solution whose initial concentration was 25 ppm is slow, in comparison with the other solutions.

Different models were applied to the results obtained in the kinetics of MB adsorption on the surface of the biomass studied. The pseudo-first-order model can describe the initial phase and the progress of the adsorption process; the pseudo-second-order equation describes that the chemisorption controls the speed of this process; According to the intraparticle diffusion model, several mechanisms are involved in the adsorption process, and this process can be described in three steps: external surface adsorption, intraparticle diffusion that is the speed-limiting step, and the final equilibrium that is very fast [46].

Next, the order in which the studied kinetic models were adjusted to the bioadsorption data obtained experimentally is mentioned.

Pseudo-second-order > Elovich > film diffusion = pseudo-first-order > intraparticle diffusion > modified pseudo-first-order.

Figure 5 shows the pseudo-second-order and Elovich isotherms obtained by adjusting the data kinetic experiments to these models; as can be seen, both models have a high correlation and therefore can describe the adsorption mechanism of methylene blue on the surface of *D. antarctica* algae.

In Table 2, it is observed that regardless of the value of the initial concentration of MB in the range studied, all bioadsorption data were adjusted to the pseudo-second-order model, this being the only model in which all the values of R^2 were above 0.95. P or which the initial adsorption rate depends exponentially on the concentration of methylene blue. The fact that this process is accurately described by a pseudo-second-order model further indicates that film diffusion, intraparticle diffusion, and surface adsorption coexisted during the adsorption of MB on the surface of the biomass, all of which factors affected the adsorption process and influence that the adsorption kinetics present the best fit when applying this model [47].

Given that the pseudo-second-order model presented the best fit of the data obtained, the value of q_e was determined, using this model; as can be seen in Table 2, the adsorption capacity values obtained experimentally are quite close to the values obtained theoretically.

The Elovich model presents the second best fit to the data obtained; this model occurs when the adsorption processes involve the chemisorption in the solid surface, and the speed of adsorption decreases with time due to the coverage of the surface layer [48]. The other models studied have a lower adjustment to the data studied, so it cannot explain with the same reliability the adsorption process that is being carried out.

To determine with greater precision the adjustment of the data obtained to the pseudo-second-order and Elovich kinetic models, five types of additional errors were determined. Table 3 reports the model that presents the best fit according to the type of error determined and the value of the initial concentration of methylene blue.

Regardless of the error studied, the best adjustment to the initial concentrations of MB of 200, 150, and 50 ppm is

Table 2: Adsorption kinetic parameters obtained by adsorption of MB onto *D. antarctica*.

Kinetic model	Parameter	Initial concentration of MB (mg/L)				
	r	25	50	100	150	200
Pseudo-first-order	K_1	0.00967	0.00783	0.00967	0.00921	0.00990
	R^2	0.986	0.952	0.893	0.937	0.992
Pseudo-second-order	K_2	0.00178	0.000287	0.000385	0.000234	0.0000730
	q_e, exp.	22.565	41.221	87.754	141.763	191.294
	q_e, cal.	22.402	40.003	86.024	140.955	196.349
	R^2	0.999	0.972	0.995	0.999	0.994
Modified pseudo-first-order	K_m	0.008	0.0059	0.0081	0.0074	0.0078
	R^2	0.985	0.875	0.839	0.971	0.991
Elovich	α	3.908	1.634	15.783	11.672	7.450
	β	0.272	0.122	0.0733	0.0356	0.0224
	R^2	0.991	0.943	0.992	0.967	0.970
Intraparticle diffusion	k_i	4.547	2.212	17.519	13.766	3.259
	R^2	0.963	0.996	0.949	0.914	0.897
Film diffusion	A	0.346	0.0591	0.212	0.416	0.0664
	k_f	0.0097	0.0078	0.0096	0.0092	0.01
	R^2	0.986	0.952	0.893	0.937	0.992

Table 3: Kinetic model that presents the best adjustment according to the initial concentration of MB and the type of error determined.

Error function	Initial concentration of MB (mg/L)				
	25	50	100	150	200
RMSE	Elovich	Pseudo-second-order	Elovich	Pseudo-second-order	Pseudo-second-order
X^2	Elovich	Pseudo-second-order	Elovich	Pseudo-second-order	Pseudo-second-order
ERRSQ	Elovich	Pseudo-second-order	Elovich	Pseudo-second-order	Pseudo-second-order
HYBRD	Elovich	Pseudo-second-order	Elovich	Pseudo-second-order	Pseudo-second-order
MPSD	Elovich	Pseudo-second-order	Elovich	Pseudo-second-order	Pseudo-second-order

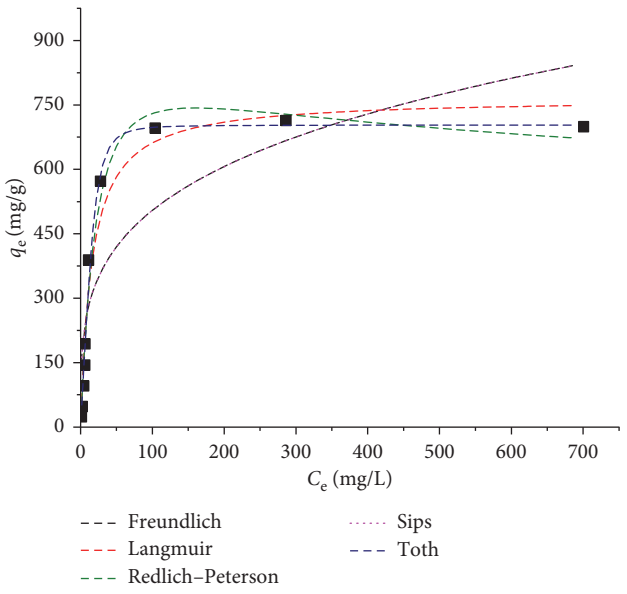

Figure 6: Bioadsorption models of methylene blue in *D. antarctica* biomass at 18 hours.

Table 4: Parameters of the models of the Freundlich, Redlich–Peterson, Sips, and Toth isotherms for the adsorption of MB on the surface of *D. antarctica*.

Models	Parameters	MB
Freundlich	K_f	148.309
	n_f	3.762
	R^2	0.873
Langmuir	Q_m	765.750
	K	0.064
	R^2	0.980
Redlich–Peterson	K_{RP}	38.133
	α_{RP}	0.022
	g	1.139
	R^2	0.989
Sips	Q_m	148.311
	K_s	−31.367
	n_s	0.266
	R^2	0.873
Toth	Q_m	702.911
	b_{T_0}	3735.703
	n_{T_0}	2.633
	R^2	0.995

given in the pseudo-second-order model, while at 100 and 25 ppm, the Elovich model presents the best correlation. It can be deduced that, at high initial concentrations, the obtained data are adjusted to the pseudo-second-order model given that the adsorption speed is related to the value of the initial concentration.

Table 5: Comparison of the adsorption capacity of MB on the surface of the biomass obtained from the algae *D. antarctica* and other compounds.

Compound	q_e (mg/g)	T (°C)	Concentration range (mg/L)	Time (min)	Reference
Mesoporous activated carbon	200.0	30	25–250	1440	[49]
GO/silicates	230	20	40–120	100	[50]
Nonionic surfactant modified montmorillonite	740.7	25	100	180	[51]
Fe_3O_4@SiO_2@CS-TETA-GO	529.1	30	1000	20	[11]
Cellulose nanocrystal	217.4	30	50–400	300	[52]
TDAW	285.7	25	40–1000	120	[53]
κ-carrageenan/graphene oxide gel beads	658.4	25	100–800	1440	[54]
Chitosan flakes	143.5	50	25–400	420	[4]
Algae *Gelidium*	171		40–800	160	[55]
Defatted algal biomass	7.8	25	1–5	60	[56]
Defatted *Laminaria japonica* biomass modified by sulfuric acid	549.45	35	20–250	60	[57]
Durvillaea antarctica	702.9	25	25–1400	540	This work

3.4. Bioadsorption Isotherms. Figure 6 shows the data of C_e and q_e obtained when determining the bioadsorption capacity of MB on the surface of the biomass obtained from the algae *D. antarctica*; in this figure, the graphs are obtained by adjusting the data of bioadsorption to the models of Freundlich, Langmuir, Redlich–Peterson, Sips, and Toth.

The best fit to the data obtained by the bioadsorption of MB on the surface of the biomass obtained from the algae *D. antarctica* is given by applying the Toth model, which indicates that the adsorption occurs on a heterogeneous surface that consists of multiple layers. This also agrees with the good fit presented by the kinetic data when applying the Elovich model since this model also describes the adsorption of the contaminant on a heterogeneous surface.

The values of the parameters obtained by adjusting the methylene blue adsorption data on the surface of *D. antarctica* biomass to the bioadsorption models studied are presented in Table 4.

The Langmuir model presented the second best fit to the data obtained in this biosorption process, and this equation is valid for systems where the biosorption occurs on a homogeneous surface.

The best fit to the obtained data is in a three-parameter model that describes that the adsorption occurs on a heterogeneous surface in multiple layers and in a model of two parameters that describe an adsorption process on a homogeneous surface. It is mainly due to the fact that the surface of the biomass has an irregular surface in which there are areas where the pores are homogeneously distributed and others in which the surface has no porosity; this agrees with the analysis of the SEM micrographs that were presented in Section 3.1.

The value of Q_e when applying the Toth model is 702.91 mg/g. This shows that the capacity of bioadsorption of MB on the surface of the biomass is high in comparison with other works reported in the literature. The exponent of the isotherm of this model (n_{T_0}) is related to the heterogeneity of the surfaces, and if it is equal to unity, the Toth model is reduced to the Langmuir model [35]. In these biosorption experiments, it was found that the value of this constant is 2.63; this value is different from one, which corroborates that this adsorption does not conform to the Langmuir model, and therefore, the majority of active sites are distributed heterogeneously. The Sips and Redlich–Peterson models are of three parameters and present characteristics of the models of Langmuir (homogeneous) and Freundlich (heterogeneous). The correlation coefficient when adjusting these statistical models to the bioadsorption data obtained was 0.873 and 0.989, respectively; these values are below the value of the correlation coefficient when applying the Toth and Langmuir models corresponding to 0.995 and 0.980, respectively. However, the value of R^2 when applying the Redlich–Peterson model is high, which suggests that the adsorption does not occur in an ideal monolayer, corroborating that this adsorption process occurred in multilayers as described by the Toth model.

Although the value of R^2 when applying the Sips model is small (0.873), the value of the constant n_s corresponding to 0.266 is closer to zero than to one, which corroborates that most active sites on the surface of the biomass which are involved in this adsorption process are distributed heterogeneously.

The value of R^2 when applying the Freundlich model was 0.873. This value is small; however, it should be noted that the value of the constant n_f when applying this model was 3.76, and according to the theory of this model, when the value of this constant is between 2 and 10, the adsorption capacity of the contaminant by the adsorbent is high [30]. This statement is corroborated when comparing the values of the methylene blue adsorption capacity presented in Table 5 for some adsorbents reported in the literature and the biomass obtained from the algae *D. antarctica*.

4. Conclusions

The bioadsorption capacity of the contaminant on the surface of the biomass increases with increasing pH, always when working at acid pH value intervals. Since the MB solution is at basic pH values, the MB adsorption capacity remains constant; in addition to this, it was determined that, in initial MB concentrations above 400 ppm, the initial pH value of these solutions is basic, which is why it is necessary to make modifications of the pH value which increase the efficiency of this process.

The pseudo-second-order model presented the best fit to the data obtained from the adsorption kinetics of MB on the surface of the biomass obtained from algae *D. antarctica*, which shows that the adsorption speed of this process is proportional to the exponential form of the initial concentration of MB present in the solution and to the time that has elapsed since the beginning of this process, as long as it is not greater than 540 min.

The Toth model presented the best fit to the data obtained from bioadsorption. By this model, it was determined that the adsorption capacity of MB on the surface of the biomass is 702.9 mg/g; this demonstrates the high efficiency that this material possesses to adsorb this contaminant.

Data Availability

Some data used to support the findings of this study are included in the tables and graphs within the article. More data (Origin and Excel files, as well as unedited images) are available from the corresponding author upon request.

Conflicts of Interest

The authors declare that there are no conflicts of interest.

Acknowledgments

The authors thank the Framework Agreement between the Universidad de los Andes and the Universidad Nacional de Colombia and the act of agreement established between the Chemistry Departments of the two universities. The authors also appreciate the grant for the funding of research programs for Associate Professors, Full Professors, and Emeritus Professors, announced by the Faculty of Sciences of the Universidad de los Andes (Colombia), 11-28-2017, 2018-2019, according to the project "Thermodynamic Characterization of the Adsorption of Contaminants on Porous Adsorbents." This work was financed by the Department of Chemistry and the Faculty of Sciences of the Andes University.

References

[1] F. Marrakchi, W. A. Khanday, M. Asif, and B. H. Hameed, "Cross-linked chitosan/sepiolite composite for the adsorption of methylene blue and reactive orange 16," *International Journal of Biological Macromolecules*, vol. 93, pp. 1231–1239, 2016.

[2] S. Thakur, S. Pandey, and O. A. Arotiba, "Development of a sodium alginate-based organic/inorganic superabsorbent composite hydrogel for adsorption of methylene blue," *Carbohydrate Polymers*, vol. 153, pp. 34–46, 2016.

[3] D. Pathania, S. Sharma, and P. Singh, "Removal of methylene blue by adsorption onto activated carbon developed from *Ficus carica* bast," *Arabian Journal of Chemistry*, vol. 10, pp. S1445–S1451, 2017.

[4] F. Marrakchi, M. J. Ahmed, W. A. Khanday, M. Asif, and B. H. Hameed, "Mesoporous-activated carbon prepared from chitosan flakes via single-step sodium hydroxide activation for the adsorption of methylene blue," *International Journal of Biological Macromolecules*, vol. 98, pp. 233–239, 2017.

[5] M. Heidarizad and S. S. Şengör, "Synthesis of graphene oxide/magnesium oxide nanocomposites with high-rate adsorption of methylene blue," *Journal of Molecular Liquids*, vol. 224, pp. 607–617, 2016.

[6] S. Aslam, J. Zeng, F. Subhan et al., "In situ one-step synthesis of Fe_3O_4@MIL-100(Fe) core-shells for adsorption of methylene blue from water," *Journal of Colloid and Interface Science*, vol. 505, pp. 186–195, 2017.

[7] S. M. Miraboutalebi, S. K. Nikouzad, M. Peydayesh, N. Allahgholi, L. Vafajoo, and G. McKay, "Methylene blue adsorption via maize silk powder: kinetic, equilibrium, thermodynamic studies and residual error analysis," *Process Safety and Environmental Protection*, vol. 106, pp. 191–202, 2017.

[8] H. Aysan, S. Edebali, C. Ozdemir, M. Ceĭik Karakaya, and N. Karakaya, "Use of chabazite, a naturally abundant zeolite, for the investigation of the adsorption kinetics and mechanism of methylene blue dye," *Microporous and Mesoporous Materials*, vol. 235, pp. 78–86, 2016.

[9] Q. Huang, M. Liu, J. Chen et al., "Marrying the mussel inspired chemistry and Kabachnik–Fields reaction for preparation of SiO_2 polymer composites and enhancement removal of methylene blue," *Applied Surface Science*, vol. 422, pp. 17–27, 2017.

[10] X.-P. Luo, S.-Y. Fu, Y.-M. Du, J.-Z. Guo, and B. Li, "Adsorption of methylene blue and malachite green from aqueous solution by sulfonic acid group modified MIL-101," *Microporous and Mesoporous Materials*, vol. 237, pp. 268–274, 2017.

[11] F. Wang, L. Zhang, Y. Wang, X. Liu, S. Rohani, and J. Lu, "Fe_3O_4@SiO_2@CS-TETA functionalized graphene oxide for the adsorption of methylene blue (MB) and Cu(II)," *Applied Surface Science*, vol. 420, pp. 970–981, 2017.

[12] N. Tahir, H. N. Bhatti, M. Iqbal, and S. Noreen, "Biopolymers composites with peanut hull waste biomass and application for Crystal Violet adsorption," *International Journal of Biological Macromolecules*, vol. 94, pp. 210–220, 2017.

[13] H. Cid, C. Ortiz, J. Pizarro et al., "Characterization of copper (II) biosorption by brown algae *Durvillaea antarctica* dead biomass," *Adsorption*, vol. 21, no. 8, pp. 645–658, 2015.

[14] M. A. Hossain, H. H. Ngo, W. S. Guo, and T. Setiadi, "Adsorption and desorption of copper(II) ions onto garden grass," *Bioresource Technology*, vol. 121, pp. 386–395, 2012.

[15] H. I. Inyang, A. Onwawoma, and S. Bae, "The Elovich equation as a predictor of lead and cadmium sorption rates on contaminant barrier minerals," *Soil and Tillage Research*, vol. 155, pp. 124–132, 2016.

[16] S. Lagergren, "About the theory of so-called adsorption of soluble substances, Kungliga Svenska Vetenskapsakad," *Handlingar*, vol. 24, pp. 1–39, 1898.

[17] Y. S. Ho and G. McKay, "Pseudo-second order model for sorption processes," *Process Biochemistry*, vol. 34, no. 5, pp. 451–465, 1999.

[18] J.-P. Simonin, "On the comparison of pseudo-first order and pseudo-second order rate laws in the modeling of adsorption kinetics," *Chemical Engineering Journal*, vol. 300, pp. 254–263, 2016.

[19] A. E. Rodrigues and C. M. Silva, "What's wrong with Lagergreen pseudo first order model for adsorption kinetics?," *Chemical Engineering Journal*, vol. 306, pp. 1138–1142, 2016.

[20] A. E. Ofomaja, E. B. Naidoo, and S. J. Modise, "Dynamic studies and pseudo-second order modeling of copper(II) biosorption onto pine cone powder," *Desalination*, vol. 251, no. 1–3, pp. 112–122, 2010.

[21] X. Yang and B. Al-Duri, "Kinetic modeling of liquid-phase adsorption of reactive dyes on activated carbon," *Journal of*

Colloid and Interface Science, vol. 287, no. 1, pp. 25–34, 2005.

[22] M. Baghdadi, "UT (University of Tehran) isotherm as a novel and useful adsorption isotherm for investigation of adsorptive removal of pollutants," *Journal of Environmental Chemical Engineering*, vol. 5, no. 2, pp. 1906–1919, 2017.

[23] C. Rill, Z. I. Kolar, G. Kickelbick, H. T. Wolterbeek, and J. A. Peters, "Kinetics and thermodynamics of adsorption on hydroxyapatite of the [160Tb] terbium complexes of the bone-targeting ligands DOTP and BPPED," *Langmuir*, vol. 25, no. 4, pp. 2294–2301, 2009.

[24] H. Uslu and S. Majumder, "Adsorption studies of lactic acid by polymeric adsorbent amberlite XAD-7: equilibrium and kinetics," *Journal of Chemical & Engineering Data*, vol. 62, no. 4, pp. 1501–1506, 2017.

[25] H. Zhang, Y. Wang, P. Bai, X. Guo, and X. Ni, "Adsorptive separation of acetic acid from dilute aqueous solutions: adsorption kinetic, isotherms, and thermodynamic studies," *Journal of Chemical & Engineering Data*, vol. 61, no. 1, pp. 213–219, 2015.

[26] J. Chen, H. Yang, and Z. Ring, "Study of intra-particle diffusion effect on hydrodesulphurization of dibenzothiophenic compounds," *Catalysis Today*, vol. 109, no. 1–4, pp. 93–98, 2005.

[27] A. Okoye, P. Ejikeme, and O. Onukwuli, "Lead removal from wastewater using fluted pumpkin seed shell activated carbon: adsorption modeling and kinetics," *International Journal of Environmental Science & Technology*, vol. 7, no. 4, pp. 793–800, 2010.

[28] E. M. Kalhori, T. J. Al-Musawi, E. Ghahramani, H. Kazemian, and M. Zarrabi, "Enhancement of the adsorption capacity of the light-weight expanded clay aggregate surface for the metronidazole antibiotic by coating with MgO nanoparticles: studies on the kinetic, isotherm, and effects of environmental parameters," *Chemosphere*, vol. 175, pp. 8–20, 2017.

[29] N. Barka, K. Ouzaouit, M. Abdennouri, and M. E. Makhfouk, "Dried prickly pear cactus (*Opuntia ficus indica*) cladodes as a low-cost and eco-friendly biosorbent for dyes removal from aqueous solutions," *Journal of the Taiwan Institute of Chemical Engineers*, vol. 44, no. 1, pp. 52–60, 2013.

[30] M. Brdar, M. Šćiban, A. Takači, and T. Došenović, "Comparison of two and three parameters adsorption isotherm for Cr(VI) onto Kraft lignin," *Chemical Engineering Journal*, vol. 183, pp. 108–111, 2012.

[31] G. McKay, A. Mesdaghinia, S. Nasseri, M. Hadi, and M. Solaimany Aminabad, "Optimum isotherms of dyes sorption by activated carbon: fractional theoretical capacity & error analysis," *Chemical Engineering Journal*, vol. 251, pp. 236–247, 2014.

[32] F. Deniz and E. T. Ersanli, "Simultaneous bioremoval of two unsafe dyes from aqueous solution using a novel green composite biosorbent," *Microchemical Journal*, vol. 128, pp. 312–319, 2016.

[33] S. Chatterjee, M. W. Lee, and S. H. Woo, "Adsorption of congo red by chitosan hydrogel beads impregnated with carbon nanotubes," *Bioresource Technology*, vol. 101, no. 6, pp. 1800–1806, 2010.

[34] A. Bera, T. Kumar, K. Ojha, and A. Mandal, "Adsorption of surfactants on sand surface in enhanced oil recovery: isotherms, kinetics and thermodynamic studies," *Applied Surface Science*, vol. 284, pp. 87–99, 2013.

[35] S. Rangabhashiyam, N. Anu, M. S. Giri Nandagopal, and N. Selvaraju, "Relevance of isotherm models in biosorption of pollutants by agricultural byproducts," *Journal of Environmental Chemical Engineering*, vol. 2, no. 1, pp. 398–414, 2014.

[36] D.-q Li, J. Wang, Z.-g Guo, J. Li, and J. Shuai, "Pectin gels cross-linked by Ca^{2+}: an efficient material for methylene blue removal," *Journal of Molecular Liquids*, vol. 238, pp. 36–42, 2017.

[37] J. Pang, F. Fu, Z. Ding, J. Lu, N. Li, and B. Tang, "Adsorption behaviors of methylene blue from aqueous solution on mesoporous birnessite," *Journal of the Taiwan Institute of Chemical Engineers*, vol. 77, pp. 168–176, 2017.

[38] F. Marrakchi, M. Auta, W. A. Khanday, and B. H. Hameed, "High-surface-area and nitrogen-rich mesoporous carbon material from fishery waste for effective adsorption of methylene blue," *Powder Technology*, vol. 321, pp. 428–434, 2017.

[39] S. Anisuzzaman, C. G. Joseph, D. Krishnaiah, A. Bono, and L. Ooi, "Parametric and adsorption kinetic studies of methylene blue removal from simulated textile water using durian (*Durio zibethinus* Murray) skin," *Water Science and Technology*, vol. 72, no. 6, pp. 896–907, 2015.

[40] D. L. Postai, C. A. Demarchi, F. Zanatta, D. C. C. Melo, and C. A. Rodrigues, "Adsorption of rhodamine B and methylene blue dyes using waste of seeds of *Aleurites moluccana*, a low cost adsorbent," *Alexandria Engineering Journal*, vol. 55, no. 2, pp. 1713–1723, 2016.

[41] A. Naskar and R. Majumder, "Understanding the adsorption behaviour of acid yellow 99 on *Aspergillus niger* biomass," *Journal of Molecular Liquids*, vol. 242, pp. 892–899, 2017.

[42] L. Giraldo, V. García, and J. C. Moreno, "Caracterización superficial en fase gas y líquida de carbones activados," *Revista de Ingeniería*, vol. 27, pp. 07–16, 2008.

[43] R. Pandimurugan and S. Thambidurai, "Synthesis of seaweed-ZnO-PANI hybrid composite for adsorption of methylene blue dye," *Journal of Environmental Chemical Engineering*, vol. 4, no. 1, pp. 1332–1347, 2016.

[44] S. Zhang, Z. Wang, Y. Zhang, H. Pan, and L. Tao, "Adsorption of methylene blue on organosolv lignin from rice straw," *Procedia Environmental Sciences*, vol. 31, pp. 3–11, 2016.

[45] W. Gao, S. Zhao, H. Wu, W. Deligeer, and S. Asuha, "Direct acid activation of kaolinite and its effects on the adsorption of methylene blue," *Applied Clay Science*, vol. 126, pp. 98–106, 2016.

[46] L.-g. Yan, L.-l. Qin, H.-q. Yu, S. Li, R.-r. Shan, and B. Du, "Adsorption of acid dyes from aqueous solution by CTMAB modified bentonite: kinetic and isotherm modeling," *Journal of Molecular Liquids*, vol. 211, pp. 1074–1081, 2015.

[47] S. Fan, Y. Wang, Z. Wang, J. Tang, J. Tang, and X. Li, "Removal of methylene blue from aqueous solution by sewage sludge-derived biochar: adsorption kinetics, equilibrium, thermodynamics and mechanism," *Journal of Environmental Chemical Engineering*, vol. 5, no. 1, pp. 601–611, 2017.

[48] J. S. Piccin, G. L. Dotto, M. L. Vieira, and L. A. Pinto, "Kinetics and mechanism of the food dye FD&C Red 40 adsorption onto chitosan," *Journal of Chemical & Engineering Data*, vol. 56, no. 10, pp. 3759–3765, 2011.

[49] M. A. Islam, M. J. Ahmed, W. A. Khanday, M. Asif, and B. H. Hameed, "Mesoporous activated coconut shell-derived hydrochar prepared via hydrothermal carbonization-NaOH activation for methylene blue adsorption," *Journal of Environmental Management*, vol. 203, pp. 237–244, 2017.

[50] P. Chen, Z.-f. Cao, X. Wen et al., "*In situ* nano-silicate functionalized graphene oxide composites to improve MB removal," *Journal of the Taiwan Institute of Chemical Engineers*, vol. 81, pp. 87–94, 2017.

[51] G. Wang, S. Wang, Z. Sun, S. Zheng, and Y. Xi, "Structures of nonionic surfactant modified montmorillonites and their enhanced adsorption capacities towards a cationic organic dye," *Applied Clay Science*, vol. 148, pp. 1–10, 2017.

[52] X. Yang, H. Liu, F. Han, S. Jiang, L. Liu, and Z. Xia, "Fabrication of cellulose nanocrystal from *Carex meyeriana* Kunth and its application in the adsorption of methylene blue," *Carbohydrate Polymers*, vol. 175, pp. 464–472, 2017.

[53] Z. Anfar, R. El Haouti, S. Lhanafi, M. Benafqir, Y. Azougarh, and N. El Alem, "Treated digested residue during anaerobic co-digestion of Agri-food organic waste: methylene blue adsorption, mechanism and CCD-RSM design," *Journal of Environmental Chemical Engineering*, vol. 5, no. 6, pp. 5857–5867, 2017.

[54] M. Yang, X. Liu, Y. Qi, W. Sun, and Y. Men, "Preparation of κ-carrageenan/graphene oxide gel beads and their efficient adsorption for methylene blue," *Journal of Colloid and Interface Science*, vol. 506, pp. 669–677, 2017.

[55] V. J. Vilar, C. M. Botelho, and R. A. Boaventura, "Methylene blue adsorption by algal biomass based materials: biosorbents characterization and process behaviour," *Journal of hazardous materials*, vol. 147, no. 1-2, pp. 120–132, 2007.

[56] T. S. Chandra, S. Mudliar, S. Vidyashankar et al., "Defatted algal biomass as a non-conventional low-cost adsorbent: surface characterization and methylene blue adsorption characteristics," *Bioresource technology*, vol. 184, pp. 395–404, 2015.

[57] H. Shao, Y. Li, L. Zheng, T. Chen, and J. Liu, "Removal of methylene blue by chemically modified defatted brown algae *Laminaria japonica*," *Journal of the Taiwan Institute of Chemical Engineers*, vol. 80, pp. 525–532, 2017.